

UNCLASSIFIED

Defense Technical Information Center
Compilation Part Notice

ADP017228

TITLE: Rectenna Arrays for Recycling Statistical Broadband Radiation

DISTRIBUTION: Approved for public release, distribution unlimited

This paper is part of the following report:

TITLE: Proceedings of the 2003 Antenna Applications Symposium [27th]
Held in Monticello, Illinois on 17-19 September 2003. Volume 1

To order the complete compilation report, use: ADA429122

The component part is provided here to allow users access to individually authored sections of proceedings, annals, symposia, etc. However, the component should be considered within the context of the overall compilation report and not as a stand-alone technical report.

The following component part numbers comprise the compilation report:

ADP017225 thru ADP017237

UNCLASSIFIED

Rectenna Arrays for Recycling Statistical Broadband Radiation

Joseph A. Hagerty, Zoya Popovic
Department of Electrical and Computer Engineering
University of Colorado at Boulder, Boulder CO 80309
zoya@colorado.edu

This paper discusses a study of rectification of broadband statistically time-varying low-power microwave radiation. Polarization, spectral content and power levels of incident radiation of the array are allowed to vary randomly over a broad range. The applications for this work are in wireless powering of indoor industrial sensors, sensor arrays in areas of low solar radiation, and recycling of ambient RF energy. A 64-element dual-polarized spiral rectenna array is designed and characterized over a frequency range of 2-18GHz. In the design, nonlinear harmonic balance simulations are combined with full-wave field analysis. The nonlinear simulations are compared with source-pull diode nonlinear measurements in order to establish a reliable design methodology. The rectifier diodes are directly matched to the antenna over a broad frequency range and a large range of input power density levels from 10^{-5} to 10^{-1} mW/cm². This eliminates matching and filtering circuits, thereby maximizing effective area. The rectified DC power and efficiency are characterized as a function of DC load impedance and DC circuit topology, polarization, incident power density, and incidence angle.

1. INTRODUCTION

Rectification of microwave signals for supplying DC power through wireless transmission has been proposed and researched in the context of high power beaming since the 1950's, a good review of which is given in [1]. In microwave power transmission, the antennas have well-defined polarization and high rectification efficiency enabled by single-frequency, high microwave power densities incident on an array of antennas and rectifying circuits. Applications for this type of power transfer have been proposed for helicopter powering [1], solar-powered satellite-to-ground transmission [2], inter-satellite power transmission [3] [4] including utility power satellites [5], mechanical actuators for space-based telescopes [6], small DC motor driving [7], and short range wireless power

transfer, e.g. between two parts of a satellite. Both linear [8], [9] dual-linear [6], [10] and circular polarization [2], [11] of the receiving antennas were used for demonstrations of efficiencies ranging from around 85-90% at lower microwave frequencies to around 60% at X-band and around 40% at Ka-band [5].

In the above referenced work, rectification was performed for narrow-band, essentially single-frequency, incident microwave radiation with relatively high power densities. A survey of the typical power densities associated with high-power rectennas is given in Table 1, along with the corresponding operating rectification efficiencies. Also shown in the table are expected power densities near a typical base station tower operating at 880 and 1990 MHz [12]. The typical solar radiation level is shown for comparison.

| Topic | Power density (mW/cm ²) | Reported efficiency | Ref. | Frequency | Polarization |
|-----------------------|-------------------------------------|---------------------|-----------------|----------------|-------------------|
| 50-m from basestation | 0.0001 | | [13] | 900 MHz | Any |
| | 0.005 | 40-50% | [8] | 2.45 GHz | Linear |
| SPST-WPT | 0.1-10 | 65-92% | [3],[4] [13] | 5.8 GHz | Circular, linear |
| FCC exposure limit | 0.5 | | | 880 MHz | Any |
| FCC exposure limit | 1.5 | | | 1990 MHz | Any |
| ANSI/IEEE standard | 1 | | | 3-30GHz | Any |
| | 10 | 80% | [3] | 5.8GHz | |
| 50-V output | 25 | 52% | [6] | 8.51 GHz | Dual linear |
| Sunlight | ~100 | | | Optical | Elliptical |
| This work | 0.000015 - 0.08 | 0.1-20% | [this work] | 2-18 GHz range | Random, arbitrary |

Table 1. Typical power densities over the microwave frequency range. The power density operating points and frequencies of several rectenna designs found in the literature and their corresponding efficiencies [8], [3], [6] are given. Also shown is the range of expected power densities used in the Solar Power Satellite (SPS) and Wireless Power Transmission (WPT) applications. The range of power densities measured in this paper is indicated for comparison. Measured ambient levels in our lab (no high power equipment) are in the 10^{-6} to 10^{-5} mW/cm² range. The solar power density is shown for comparison.

Concerns have been expressed in terms of possible health hazards [13]. In [8], rectification of low power levels was discussed for battery-free transponders, with

power densities on the order of $0.01\text{mW}/\text{cm}^2$. More recently, broadband rectification of very low-power incident radiation (less than $1\text{mW}/\text{cm}^2$) was demonstrated in [14]. This paper focuses on incident power densities and input power levels that are orders of magnitude lower than those associated with the projects in the literature cited above, as shown in Table 1.

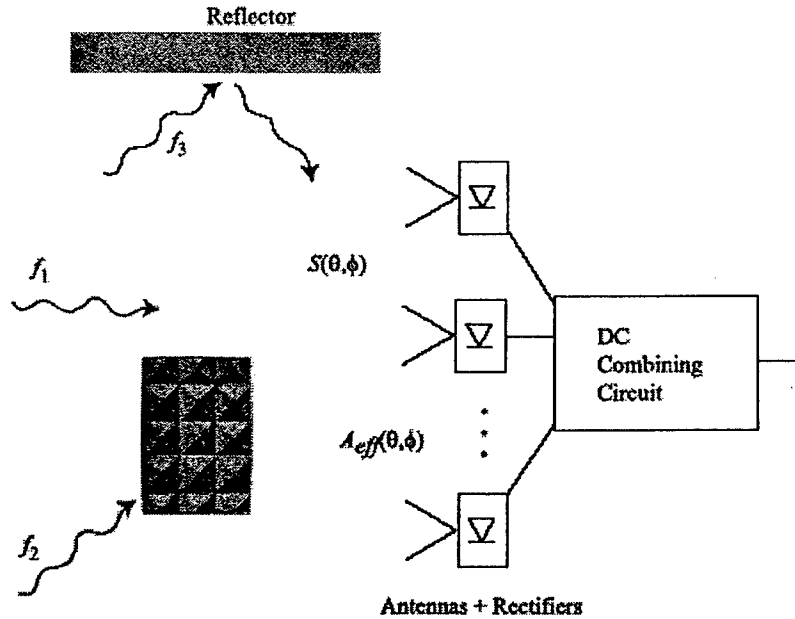


Figure 1. Block diagram of rectenna array for ambient energy recycling. Waves of different frequencies and power levels propagate through a complex environment before they are received by a dual-polarized array of antennas. Each element in the array is integrated with a rectifying device. The resulting DC outputs are combined

The general block-diagram of the rectenna array discussed in this paper is shown in Figure 1. Multiple sources of different frequencies are radiating power in all directions in a rich scattering environment. The DC powers from many rectenna elements are added by current and voltage summing with a conversion efficiency

$$\eta = P_{DC}/P_{RF},$$

which is a function of statistically varying incident RF power. The received average RF power over a range of frequencies, at any instant in time is given by

$$P_{RF}(t) = \frac{1}{f_2 - f_1} \int_{f_1}^{f_2} \int_0^{4\pi} S(\Omega, f, t) A_{eff}(\Omega, f) d\Omega df$$

where Ω is the solid angle in steradians and $S(\Omega, f, t)$ is the time varying frequency and angle dependent incident power density. A_{eff} is the angle, frequency, and polarization dependent effective area of the antenna. Because of the nonlinearity of the diode, the mismatch between the antenna and the rectifying diode is dependent on power as well as frequency. The diode is driven as a half-wave rectifier with an efficiency limited to

$$\eta_{max} = \frac{1}{1 + \frac{V_D}{2V_{out}}}$$

where V_{out} is the output DC voltage and V_D is the drop across the conducting diode. In this work it is more appropriate to measure the efficiency defined above through power, which includes the loss due to reflected power. For low power applications, as is the case for collected ambient energy, there is generally not enough power to drive the diode in a high efficiency mode. Furthermore, rectification over multiple octaves requires a different approach from standard matching techniques. In a rectenna application, the antenna itself can be used as the matching mechanism instead of using a transmission-line matching circuit as in [5]–[11]. The antenna design is therefore heavily dependent on the diode characteristics.

2. DESIGN OF INTEGRATED RECTIFIER DIODE AND ANTENNA ELEMENT

The design of a broadband nonlinear active antenna element starts with the determination of the active element impedance over a range of frequencies and power levels. This analysis is performed using nonlinear Harmonic Balance simulations in Agilent ADS with the nonlinear diode model provided by the manufacturer. Nonlinear analysis is required since the nonlinear capacitance of the diode needs to be taken into account past a few GHz for most devices. In addition, harmonics are produced by the diode and the reflected harmonic energy from the input or output side of the diode can alter the voltage across the diode. Another important effect that linear analysis cannot take into account is the fact that the diode self-biases as it produces more DC current, thus moving the DC operating point of the IV curve in a nonlinear fashion.

Figure 2 shows the range of impedances for the Schottky diode used in this work, for a frequency range from 1-16GHz and a power range from -30dBm to 10dBm. The magnitude of the optimal source impedance becomes smaller with increasing incident power. The same occurs as the DC load approaches the optimal value, however the effect is not as dramatic. More significantly, the

optimal source impedance moves counter-clockwise along a constant admittance circle with increasing frequency due to the junction capacitance. This needs to be taken into account when designing the antenna element, since most antennas have impedance traces that move clockwise with increasing frequency on the Smith chart.

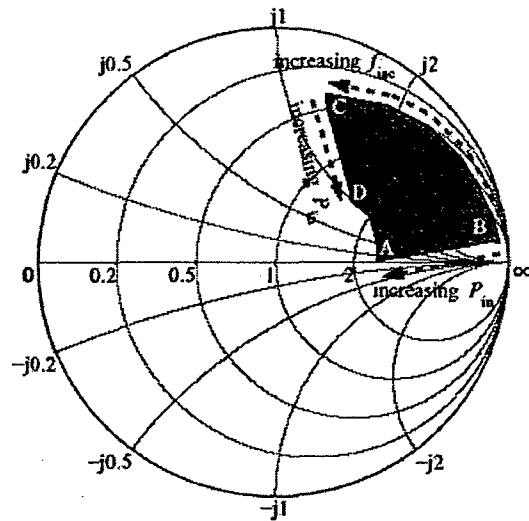


Figure 2. Simulated range of optimal source impedances for the SMS7630 Schottky diode as the incident wave frequency and input power are varied from 1 to 16 GHz and -30dBm to 10dBm, respectively. Within the shaded area, region A corresponds to high input power and low frequency, B to low power and low frequency, C to low power and high frequency, D to high power and high frequency.

In most rectenna designs, a narrow band antenna is used to feed a transmission line followed by space-consuming, traditional matching and filtering sections. In the work presented here the diode is integrated directly into the antenna, reducing the required area and increasing the bandwidth. The antenna impedance is either obtained from simulations using a full-wave solver, or by measurements, and then included in the HB simulation as the internal impedance of the power source used to drive the circuit. The major problem in broadband rectenna design lies in the nature of the antenna and diode frequency dependent impedances. For maximal power transfer, the antenna impedance would match the optimal diode impedance for all frequencies. Our approach is to present a constant impedance to the diode by using a frequency independent antenna element.

In order to verify the design method, we chose a well-known antipodal Vivaldi tapered slot antenna, Figure 3a, for which we had both simulated and measured input impedance available [15]. The packaged Schottky diode is soldered to the

microstrip feed line near the connector. Figure 3b shows the agreement between Harmonic Balance simulations using measured antenna return loss, and measurements of the DC output voltage into a 660-ohm load.

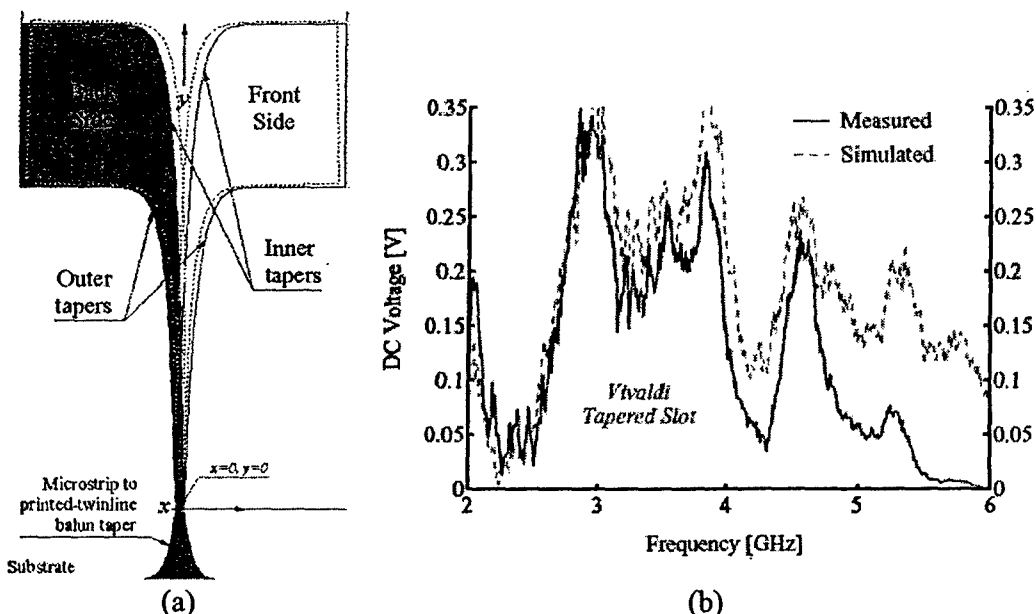


Figure 3. (a) Layout of test Vivaldi antenna. A Schottky diode is connected to the microstrip feed line, and the obtained simulated and measured DC voltage from 2 to 6 GHz is shown in (b).

For a large printed rectenna array, the tapered slot is not a convenient element. An equiangular spiral, Figure 4a, was chosen as the array element for the following reasons: (1) uniplanar with convenient feed point for diode connection, (2) possible dual polarization, (3) convenient connection of dc lines at the tips of the spiral arms. The spiral element was simulated with full-wave CAD tools (Ansoft's *Ensemble* and Zeland's *IE3D*) resulting in a one-port frequency dependent impedance that becomes the diode load in the rectenna.

The measured impedance of a passive spiral with a coaxial feed-line positioned at the center of the spiral is shown in Figure 4b. A diode is then connected at the antenna feed and the resulting rectenna element performance is shown in Figure 5. The disagreement around 4 GHz is believed to be caused by the 1-cm long unbalanced coax feed which was needed to do a single-element measurement, but does not exist in the final array.

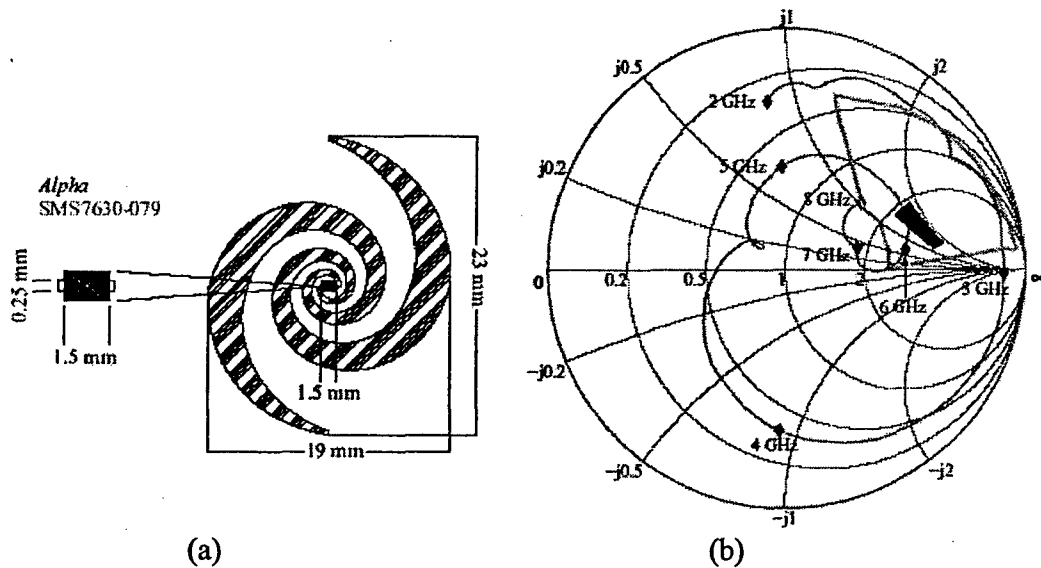


Figure 4. (a) Layout of spiral rectenna element with a packaged Schottky diode connected at the feed point. (b) Simulated input impedance of the spiral element normalized to 50 ohms. The optimal region of impedances from Figure 2 is outlined in gray, and the frequencies and range of input power levels used for this measurement are represented by the black region.

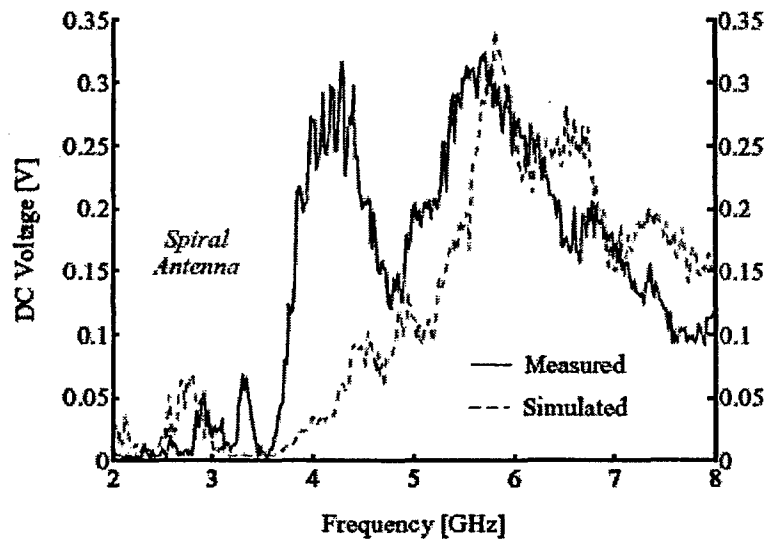


Figure 5. Measured and simulated DC voltage response of a single spiral element with an unbalanced coaxial feed used to extract the C voltage into a 600-ohm load. The disagreement at 4GHz is attributed to the unbalance feed.

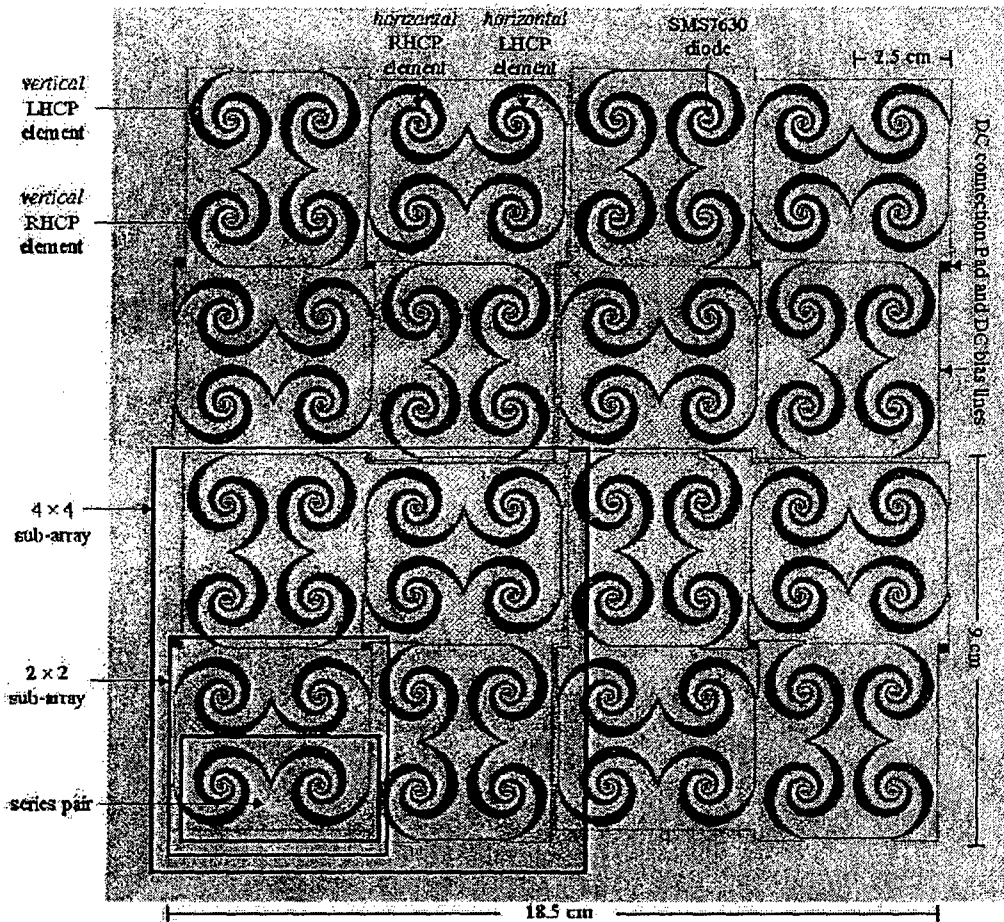


Figure 6. Layout of 64-element rectenna array with alternating RHCP and LHCP spirals.

3. RECTENNA ARRAY DESIGN AND CHARACTERIZATION

A 64-element array of left and right hand circularly polarized spiral elements, Figure 6, is designed so that each spiral element is directly connected to a rectifier diode. Therefore, the RF powers received independently by each element are summed upon rectification as DC currents and/or voltage of total rectified power from the array depends on the angle of incidence of the RF plane wave(s). The angle-dependent rectified DC power of a single element can be used to define an *element DC radiation pattern*:

$$G_{DC}(\theta, \phi) = \eta(P_{RF}) \frac{4\pi \cdot P_{RF}}{S(\theta, \phi)\lambda^2} = \eta(P_{RF})G(\theta, \phi)$$

where $G(\theta, \phi)$ is the RF radiation pattern. The DC radiation pattern, $G_{DC}(\theta, \phi)$, is different from the RF radiation pattern due to the nonlinear dependence of efficiency on RF power. The resulting pattern obtained by measuring the DC voltage across an optimal load exhibits lower gain at larger angles θ and ϕ . The radiation pattern for the n-element array is the same as the element pattern, with an additional multiplier factor that is a function of the DC connections in the array, and to first order is not a function of angle.

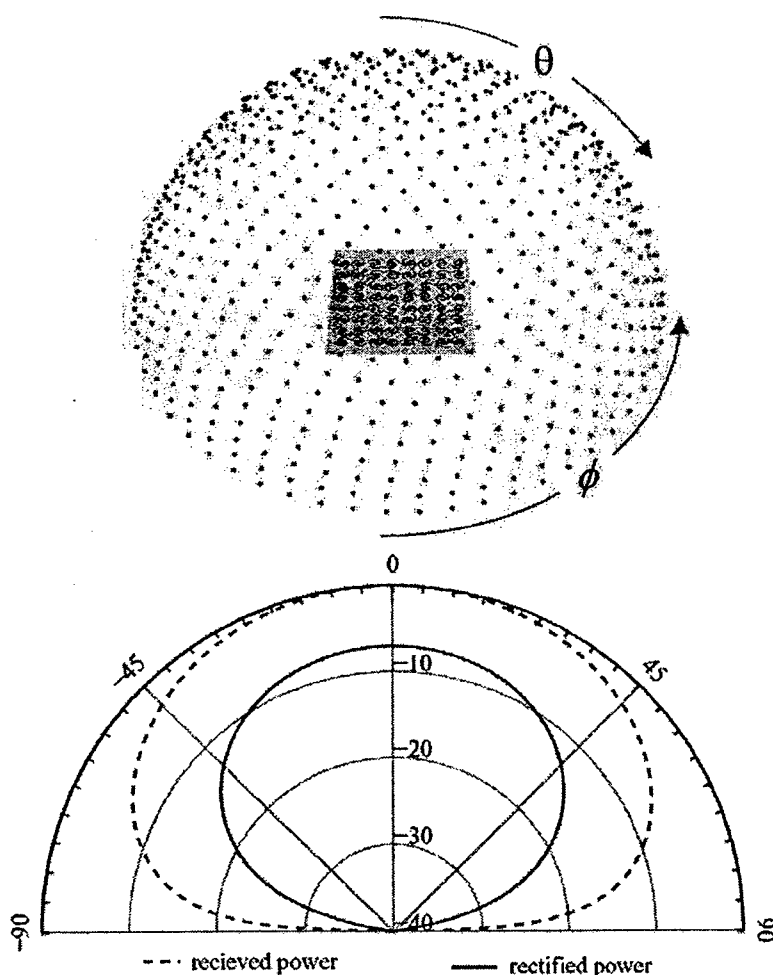


Figure 7. Layout of 1024 points from which the array was illuminated during the pattern measurements (top). Measured DC radiation pattern compared to received RF power shows the expected narrowing in pattern due to nonlinearity (bottom).

The patterns of the rectenna array are found by measuring the output DC rectified power over a hemisphere sampled at 1012 points, Figure 7a. One cross-section of a pattern is shown in Figure 7b to point out the relationship of the rectified to the actual received power by the array. Figure 8 shows measured radiation patterns, which are a superposition of the response to two orthogonally linearly polarized incident waves. This means that the array suffers an average 3 dB input polarization loss for *every* possible polarization of the incident energy. However, this strategy ensures a flat polarization response. At higher frequencies the spiral element is predominately circularly polarized. In order to design a broadband array with as uniform a pattern in space and polarization as possible, RHCP and LHCP spirals are alternated in the layout.

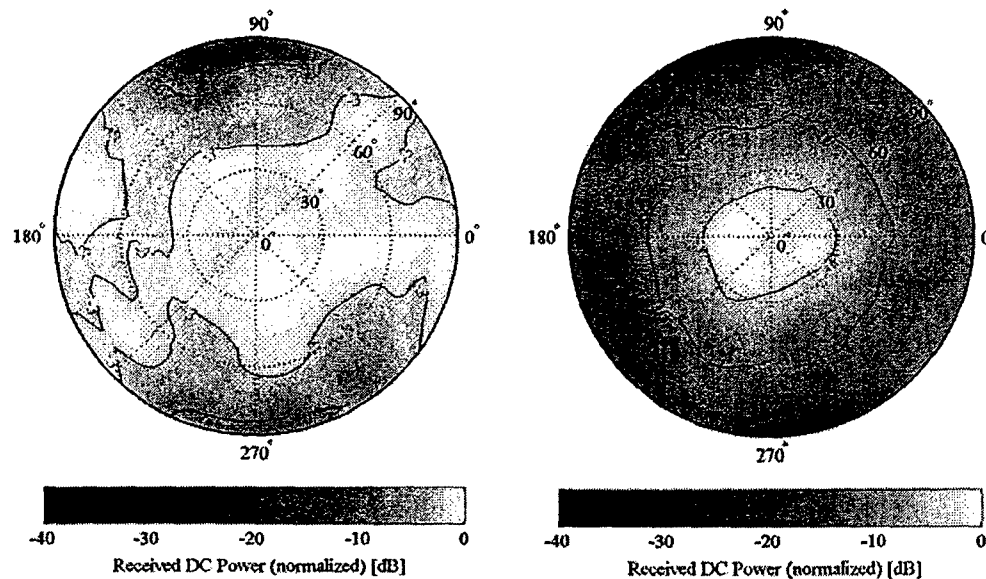


Figure 8. Measured DC power as a function of angle of incidence over a hemisphere for two orthogonally linearly polarized input waves at 2 GHz (left) and 4.6 GHz (right).

The planar layout of the array places certain limits on the polarization and reception at azimuth angles. Figure 8 shows that the radiation pattern has low directivity and is similar to that of a single element. Note that the size of the array is $1.5 \lambda_0^2$ at 2 GHz, and $116 \lambda_0^2$ at 18 GHz. However, by observing the patterns in Figure 8 it is seen that the array receives from all directions over a broad frequency range.

The crucial design step for the array is to achieve optimal DC combining efficiency. Previous work shows that predominately parallel connections (current-summing) lead to smaller matched loads for the rectenna [16]. For a series connected array (voltage-summed), the matched load is much higher. This can be seen by reducing the array to a combination of DC Thevenin sources where the matched load corresponds to the total source resistance. The nonlinear performance of the diodes must again be considered when considering the DC connections. Increased current or voltage in a predominately series or parallel-connected array can lead to over-biasing of the 64 element array is connected using 2×1 parallel pairs connected in series to form a 2×2 sub-subarray: four of these are connected in parallel to create a 4×4 subarray: four more of these are then left as units to comprise the 8×8 array with reconfigurable connectivity.

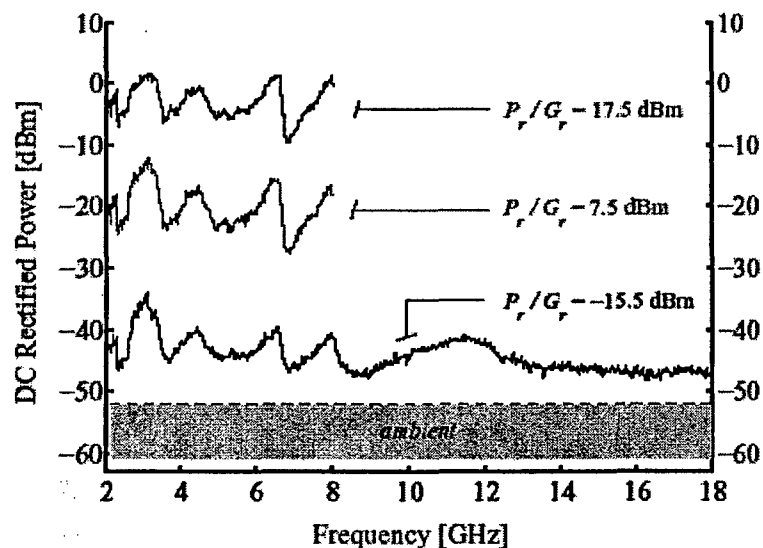


Figure 9. Measured broadband frequency response for various incident power levels related to the power density, S , by $P/G = S\lambda_0^2/(4\pi)$. The shaded area represents the range of rectified power levels resulting from ambient RF background signal present in the building.

The frequency dependence is measured in two ways: three dimensional patterns are integrated from 2 to 8 GHz where sufficient power was available for the measurement. Since the radiation patterns are reasonably smooth, only the broadside frequency response was measured. Higher input powers were used for 2 to 8 GHz and a low power level was used for the broad range from 2 to 18 GHz. The broadside frequency response was also measured using a uniform incident

power density to synthesize constant input power to the diodes. The results for three input power levels are shown in Figure 9.

4. DISCUSSION AND CONTINUED WORK

A study of reception and rectification of broadband statistically-varying rf radiation is presented in this paper. The experimental results show that the combined electromagnetic field analysis of the antenna element and harmonic balance nonlinear circuit simulations for the integrated diode result in predictable rectenna performance. The work focuses on arbitrary polarized low incident power density reception and rectification and shows that rectification efficiencies with average 20% over time, frequency and polarization are achieved. If one of these requirements is relaxed, i.e., highpower, narrow-band, linearly-polarized and/or time-constant power is transmitted, higher efficiencies up to 60% at X-band [5] can be expected. The motivation for considering the low-power multipath channel case are applications in ambient energy recycling and low-power batteryless sensors.

The first type of application addresses using otherwise wasted power, which in some cases can also help reduce health hazards. For example, the rooftops of buildings in city centers are often leased to a number of wireless providers and technical staff has reported health problems when servicing a transmitter in the presence of other operating transmitters [14]. In this environment, a variety of output powers, frequencies, and polarizations are present, and interference between a number of antennas in each other's near fields changes their radiation properties, accounting for more *wasted* power. The results of this paper show that this power can be absorbed (received), rectified and stored for future use.

It can be shown that a simple sensor that requires a small energy packet to perform the sensory function, and one packet to transmit data, it would be able to transmit new data around 20 times per second in the best case under the wireless power delivery of low power levels such as the ones described in this paper. An example of such an application is a manufacturing environment, where a large number of sensors occasionally transmit data such as stress, temperature, pressure, light level, etc. A large number of such sensors with no batteries that need replacing (or recycling) can be charged with a low-power transmitter overnight. In such an indoor multipath propagation environment, the spatial distribution of polarization and power varies statistically. The results of this paper show that it is possible to efficiently collect such energy by receiving and

rectifying two orthogonal polarizations independently and adding the power upon rectification.

Finally, a third future application of the described systems which will present a more difficult antenna design problem is delivery of low power levels to sensors implanted in live bodies. In this case, the antenna is embedded in a lossy inhomogeneous dielectric and the heating due to the limited diode efficiency and absorption of the tissue is a relevant and interesting topic of research.

ACKNOWLEDGEMENT

This work was funded by an ARO MURI in quasi-optical power combining, ITN Energy Systems, Inc., and the National Science Foundation Wireless Initiative.

REFERENCES

- [1] W.C. Brown, "The history of power transmission by radio waves," *IEEE Transactions on Microwave Theory and Techniques*, vol. 32, no. 9, pp. 1230–1242, Sept. 1984.
- [2] N. Shinohara and H. Matsumoto, "Experimental study of large rectenna array for microwave energy transmission," *IEEE Transactions on Microwave Theory and Techniques*, vol. 46, no. 3, pp. 261–267, Mar. 1998.
- [3] J.O. McSpadden, F.E. Little, M.B. Duke, and A. Ignatiev, "An in-space wireless energy transmission experiment," *IECEC Energy Conversion Engineering Conference Proceedings*, vol. 1, pp. 468–473, Aug. 1996.
- [4] Kai Chang, *Microwave Ring Circuits and Antennas*, John Wiley & Sons, New York, NY, 1996.
- [5] T. Yoo and K. Chang, "Theoretical and experimental development of 10 and 35 GHz rectennas," *IEEE Transactions on Microwave Theory and Techniques*, vol. 40, no. 6, pp. 1259–1266, June 1992.
- [6] L.W. Epp, A.R. Khan, H.K. Smith, and R.P. Smith, "A compact dualpolarized 8.51-GHz rectenna for high-voltage (50 V) actuator applications," *IEEE Transactions on Microwave Theory and Techniques*, vol. 48, no. 1, pp. 111–120, Jan. 2000.
- [7] Y. Fujino, T. Ito, M. Fujita, N. Kaya, H. Matsumoto, K. Kawabata, H. Sawada, and T. Onodera, "A driving test of a small DC motor with a rectenna array," *IEICE Trans. Commun.*, vol. E77-B, no. 4, pp. 526–528, Apr. 1994.
- [8] W.C. Brown, "An experimental low power density rectenna," *IEEE MTT-S International Microwave Symposium Digest*, pp. 197–200, 1991.

- [9] J.O McSpadden, R.M. Dickinson, L. Fan, and Kai Chang, "Design and experiments of a high-conversion-efficiency 5.8-GHz rectenna," *IEEE MTT-S International Microwave Symposium Digest*, vol. 2, pp. 1161–1164, 1998.
- [10] J.O. McSpadden and K. Chang, "A dual polarized circular patch rectifying antenna at 2.45 GHz for microwave power conversion and detection," *IEEE MTT-S International Microwave Symposium Digest*, pp. 1749–1752, 1994.
- [11] B. Strassner and K. Chang, "A circularly polarized rectifying antenna array for wireless microwave power transmission with over 78% efficiency," *IEEE MTT-S International Microwave Symposium Digest*, pp. 1535–1538, 2002.
- [12] J. C. Lin, "Radio frequency exposure and safety associated with base stations used for personal wireless communication," *IEEE Antennas and Propagation Magazine*, vol. 44, no. 1, pp. 180–183, Feb. 2002.
- [13] J. C. Lin, "Space solar-power stations, wireless power transmissions, and biological implications," *IEEE Microwave Magazine*, pp. 36–42, Mar. 2002.
- [14] J.A Hagerty and Z. Popović, "An experimental and theoretical characterization of a broadband arbitrarily-polarized rectenna array," *IEEE MTT-S International Microwave Symposium Digest*, vol. 3, pp. 1855–1858, 2001.
- [15] H. Loui, J. Peeters Weem, Z. Popovic, "A dual-band dual-polarized nested Vivaldi slot array with multilevel ground plane," *to appear in IEEE Trans. Antennas and Propagation*, Sept. 2003.
- [16] N. Shinohara and H. Matsumoto, "Dependence of dc output of a rectenna array on the method of interconnection of its array elements," *Electrical Engineering in Japan*, vol. 125, no. 1, pp. 9–17, 1998.